Chapter 8

Motile Properties of Cytoplasmic Dynein

Samara L. Reck-Peterson,[a] Ronald D. Vale,[b] and Arne Gennerich[c]

[a] *Department of Cell Biology, Harvard Medical School, Boston, MA, USA*

[b] *Department of Cellular and Molecular Pharmacology, University of California School of Medicine, San Francisco, CA, USA*

[c] *Department of Anatomy and Structural Biology and Gruss-Lipper Biophotonics Center, Albert Einstein College of Medicine, New York, NY, USA*

Samara_Reck-Peterson@hms.harvard.edu

Cytoplasmic dynein is the major minus-end-directed microtubule-based motor in nearly all eukaryotic cells. Due to its large size and subunit complexity, dissecting the motile properties of dynein has been challenging. However, recent advances in recombinant approaches to purify dynein, as well as studies with the native motors, have begun to reveal the details of how dynein steps along microtubules and responds to externally applied loads. Compared to studies on the other cytoskeletal motors, myosin and kinesin, studies of dynein are still in their infancy, leading to a number of controversies regarding the dynein motile mechanism. However, a consensus is beginning to emerge from single-molecule studies that dynein is a highly processive motor, which can take forward, backward and diagonal steps related in size to the minimum repeat unit of the microtubule (8 nm). Here we discuss some of the more controversial aspects of the dynein stepping mechanism and response to load. We also review what is known about dynein regulation by its multiple ATP-binding sites and associated cofactors, the dynactin complex, LIS1, and NudE.

8.1 INTRODUCTION

Cytoplasmic dynein (referred to as dynein in this chapter) performs nearly all minus-end-directed microtubule (MT)-based transport in eukaryotic cells. All

Handbook of Dynein
Edited by Keiko Hirose and Linda A. Amos

www.panstanford.com

eukaryotic genomes that have been sequenced contain a single cytoplasmic dynein heavy chain gene that is expressed in both ciliated and nonciliated cells, with the exception of higher plants, which have no dynein genes, but an expanded family of minus-end-directed kinesins [76]. As the major minus-end-directed transporter, dynein has a diverse set of cargo, ranging from organelles, to RNAs, to signaling proteins. Dynein also has multiple functions in cell division and migration and can be hijacked by nonphysiological cargo such as viruses [23].

In this chapter we will focus on studies of dynein motility, primarily the motile properties of the purified enzyme *in vitro*. The cytoplasmic dynein holoenzyme is composed of dimeric subunits of a motor (or head)-containing heavy chain (HC), intermediate chain (IC), light intermediate chain (LIC), and light chains (LC) [53] (Fig. 8.1). There are three LC families: TCTEX, LC7/Roadblock, and LC8, all of which are also present in two copies per holoenzyme and bind directly to the dynein IC [53]. Only the LC8 light chain is present in all organisms that also have a dynein HC gene. In addition to the holoenzyme subunits, a number of other proteins and protein complexes are required for dynein's function in cells (reviewed in [21]). In Section 8.5 we will discuss the role of those that have been shown to regulate dynein's motile properties, the dynactin complex, LIS1, and NudE.

One of the challenges for studying the motile properties of dynein has been its enormous size and complexity. While the holoenzyme alone is approximately 1.2 MDa, adding the dynactin complex, LIS1, and NudE brings the total complex size to ~2.5 MDa. The HC itself is quite complicated and distinctly different evolutionarily from the other cytoskeletal motor proteins, kinesin, and myosin. The domain structure of the HC is shown in Fig. 8.1A. Briefly, dynein's amino-terminal "tail" domain represents ~30% of the entire mass of the dynein HC and is required for dimerization and the association of most dynein subunits and associated proteins. Situated between the tail and motor domains, is a recently discovered element, the "linker" domain, which shifts position relative to the dynein motor ring during the ATPase cycle and is required for motility [2, 27, 55, 57] (Fig. 8.1B, see Chapters 3 and 4). Following the linker domain, and comprising ~60% of the mass of dynein, is the motor domain, which is made up of a hexameric ring of concatenated AAA+ ATPase domains. The first four of these AAA+ domains are expected to bind ATP or ADP based on the phenotypes of mutants [4, 28, 54, 67]. Between AAA+ domains 4 and 5 is a 10–15 nm antiparallel coiled coil "stalk" capped by the dynein microtubule-binding domain (MTBD), whose atomic structure was recently solved ([3], Chapter 6). Thus, some of the striking features of the dynein molecule in comparison to kinesin and myosin include the high number of ATP molecules that can bind per dimer (up to 8 for dynein vs. 2 for kinesin and myosin) and the large distance between the primary site of ATP hydrolysis (AAA1 in dynein) and the site of filament binding (20–25 nm for dynein vs. a few nm for myosin and kinesin).

8.2 SOURCES OF CYTOPLASMIC DYNEIN

Most studies of the motile properties of cytoplasmic dynein have been performed using either purified native or recombinant protein, although a few studies have begun to investigate the motile properties of dynein in living cells (discussed in Section 8.6). In this section we will describe the most widely used sources of both native and recombinant dynein.

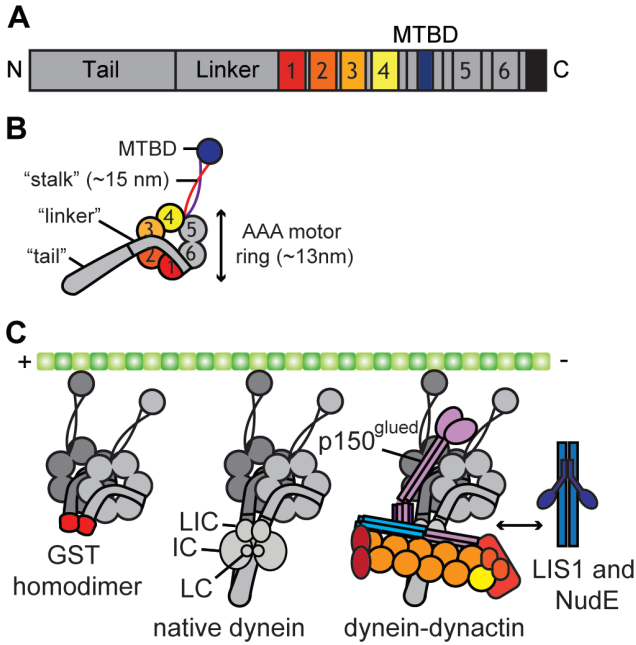

Figure 8.1 Domain structure, subunit, and cofactor composition of cytoplasmic dynein. (A) Domain structure of the dynein heavy chain. (B) Two-dimensional domain structure of the dynein heavy chain. (C) Recombinant and native dynein constructs used in motility studies reported in this chapter. From left to right: monomeric dynein artificially dimerized with GST (monomeric dynein consists of 380kDa for mammalian or *Dictyostelium* dynein and 331kDa for *S. cerevisiae* dynein); native dynein heavy chain (HC) with its associated subunits, intermediate chain (IC), light intermediate chain (LIC), and light chain (LC); and native dynein with its associated cofactors, dynactin, LIS, and NudE. The MT-binding subunit of dynactin, $p150^{Glued}$/Nip100 is shown in purple.

8.2.1 Native Dynein

Cytoplasmic dynein was originally purified from bovine brain [52, 78]. Dynein is very abundant in mammalian brain tissue, and this continues to be

an excellent source of dynein for motility studies (see [1] and Section 7.2.1 for a purification protocol). Recent work has taken advantage of a mouse strain harboring a GFP-tagged dynactin complex to purify fluorescently labeled native dynein-dynactin [58]. In our work, we use the yeast, *S. cerevisiae*, as a source of both native and recombinant dynein. Tags that aid in purification and fluorescent labeling do not disrupt dynein function *in vivo*, and thus allow the purification of full-length dynein expressed from its endogenous promoter along with its associated subunits [22, 55]. Native cytoplasmic dynein has also been purified for *in vitro* studies from *Drosophila*, *Dictyostelium*, and *Neurospora crassa* [18, 30, 65].

8.2.2 Recombinant Dynein

While native dynein sources allow researchers to study dynein in its most physiologically relevant form, dissecting how dynein generates force and motility requires a recombinant source, allowing extensive modification of the dynein gene to include mutations, truncations, deletions, and the insertion of tags for purification and labeling, as has been the case for dissecting other molecular machines. The advent of recombinant systems to study dynein in the past few years has led to a wealth of new information about dynein's mechanochemical mechanism and structure.

The first recombinant dynein was generated by expressing the full-length rat dynein cDNA in either a mammalian cell line (COS-7) or baculovirus infected insect cells [9, 40]. This recombinant dynein behaved similarly to native brain dynein in MT-gliding assays, but unlike native dynein showed poor release from MTs in the presence of Mg-ATP [9, 40]. More recently, a monomeric motor domain (380kDa) of rat cytoplasmic dynein was expressed and purified from insect cells; however, motility studies on this motor have not been reported [20]. The development of two model systems for dynein expression, *Dictyostelium* [29, 49] and *S. cerevisiae* [55], have created robust sources of recombinant dynein, in which both the manipulation and purification of the recombinant proteins have become routine. In the *Dictyostelium* system, a 380 kDa monomeric dynein has been studied extensively in ATPase and MT-gliding assays, and in a FRET-based assay to monitor conformational changes within the motor domain ([27–29], Chapter 3). In the yeast system, a number of monomeric constructs have been studied, as well as artificially dimerized monomers that behave similarly to full-length yeast dynein dimers [55] (Fig. 8.1C). Yeast dynein has been analyzed in ATPase and MT-gliding assays, and in single-molecule assays that probe both processivity and force production [4, 11, 55].

8.3 CYTOPLASMIC DYNEIN MOTILITY IN THE ABSENCE OF LOAD

The first assays used to study the motility of dynein in the absence of significant load were *in vitro* MT-gliding assays and bead-based assays (Fig. 8.2). MT-gliding assays monitor the ability of coverslip-attached motors to move MTs across the coverslip surface (Fig. 8.2A). Similarly, motor-coated latex beads can be assayed for their ability to move along coverslip-attached MTs (Fig. 8.2B). Even before the dynein gene was cloned, its motile properties had begun to be characterized using such assays [52, 77]. While

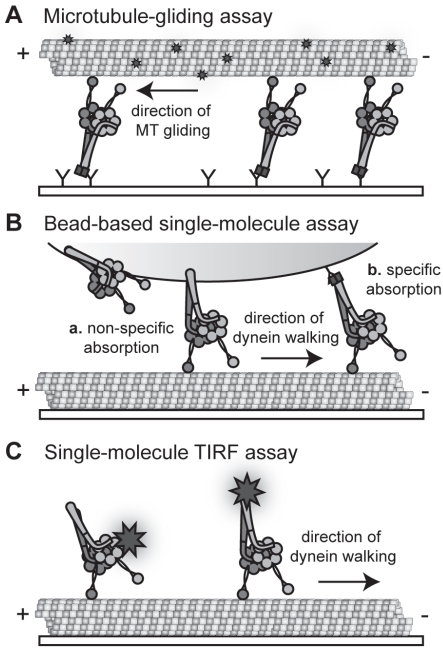

Figure 8.2 *In vitro* motility assays used to study cytoplasmic dynein. (A) MT-gliding assay. In this assay motors are linked either nonspecifically or specifically (we use antibodies to a GFP tag on the tail of dynein) to a coverslip surface. Fluorescently labeled MTs will be pushed by active motors along the surface of the coverslip, with MTs moving in the opposite direction that the motor is walking. (B) Bead-based single-molecule assay. Motors nonspecifically absorbed to beads (a) can bind in many different orientations, some of which will be competent for motility (right) and some that may not be competent for motility (left). Motors can also be absorbed specifically, shown here using antibodies to a GFP tag on the tail of dynein (b). Motor-coated beads are then observed moving along coverslip-attached MTs. (C) Single molecule total internal reflection fluorescence (TIRF) microscopy-based assay. In this assay MTs are linked to coverslips (usually using biotinylated MTs that are then coupled to streptavidin-coated surfaces) and then fluorescently labeled motors can be directly observed walking along their MT track when imaged using TIRF microscopy.

velocity measurements can vary depending on the purification method and buffer conditions used, these first studies showed that dynein powered MT movement at speeds of ~1 μm/s and that it was a minus-end-directed motor like the axonemal dyneins that had already been characterized, and thus distinct from conventional kinesin (kinesin-1).

Since the first reports on dynein motility, a number of studies have shown that dynein is a processive motor: single dynein motors are capable of taking multiple steps along MTs before releasing. In this section we will discuss these experiments as well as those that went on to characterize the stepping behavior and directionality of dynein in the absence of an applied load.

8.3.1 Cytoplasmic Dynein is a Processive Motor

The first study to demonstrate that dynein is a processive motor relied on a bead-based assay in which dynein (purified from chick brain) was absorbed to latex beads nonspecifically [80] (Fig. 8.2B, a). By studying bead motility as a function of the motor-to-bead ratio, these experiments suggested that single dynein motors are capable of driving continuous bead movement along MTs. Later experiments using bead-based assays confirmed these findings [26, 38]. More recently, the processive motion of individual fluorescently labeled dynein molecules has been directly visualized using total internal reflection fluorescence (TIRF) microscopy [55, 58, 74] (Fig. 8.2C; Fig. 8.3A). Full-length yeast cytoplasmic dynein specifically labeled with a single fluorophore at dynein's C-terminus (the end of the motor domain) showed minus-end-directed processive movement with an average run length of ~2 μm [55]. Porcine brain dynein nonspecifically labeled with quantum dots and GFP-labeled dynein-dynactin purified from mouse brain also showed processive motion in single-molecule TIRF assays [58, 74].

The first mechanistic insights came from structure-function studies that demonstrated that cytoplasmic dynein processivity requires two heads [55, 65]. Reck-Peterson *et al.* [55] examined engineered single-headed monomeric and artificially dimerized two-headed dyneins and demonstrated that only two-headed dyneins could move processively [55], suggesting that the dynein heads coordinate with each other to move processively. Indeed, Shima *et al.* [65] showed that truncated monomeric *Dictyostelium* dynein spends less time bound to MTs during its ATPase cycle than a single motor domain of a walking dimeric dynein, suggesting that, in the dimer, mechanochemical steps in one head are affected by the presence of the second head. Thus, some form of "gating" (a mechanism that stalls one head until the other head opens a "gate" that allows it to proceed through the next step in its mechanochemical cycle) must exist for dynein.

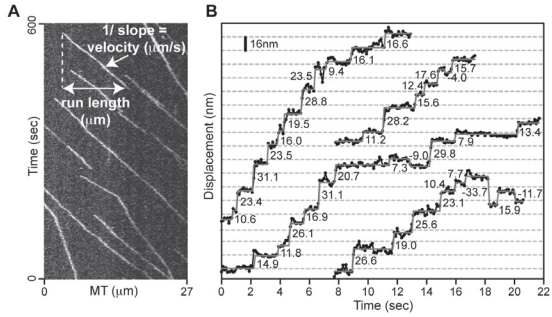

Figure 8.3 Cytoplasmic dynein is a processive motor. (A) Kymograph of moving artificially dimerized (with GST) yeast dynein covalently labeled with tetramethylrhodamine on the C-terminus of the motor domain purified from yeast strains lacking Lis1/Pac1 and NudE/Ndl1 (see [55] for more details on methods). The *y*-axis of the kymograph represents every frame of a 10 min movie (images taken every 2 s) and the *x*-axis is the length of a single MT (27 μm). Diagonal lines represent moving molecules, with velocity equal to the inverse of the slope. The run length of individual molecules can be easily determined (double headed arrow). The runs shown here are on average longer than those previously published due to using buffers with a decreased ionic strength (30 mM vs. 80 mM in the published studies [4, 55]). (B) Stepping trace of artificially dimerized yeast dynein labeled with a single quantum dot on a single-motor domain. Dynein takes variable sized steps in both the forward and backward direction. The average step size of the 34 forward steps shown here is 18.5 nm. When hundreds of steps are analyzed, the average step size of a dynein motor domain is ~16 nm [55], which is twice the step size of dynein's tail domain (~8 nm). The raw data are shown in black and the steps detected by a step finding program [24] in grey.

8.3.2 Stepping Behavior of Cytoplasmic Dynein Under Unloaded Conditions

While single-molecule studies have established that individual dimeric dynein molecules can take multiple successive steps along MTs, the details of dynein's step size and directionality remain controversial. Mallik *et al.* [38] first reported that plastic beads bound nonspecifically to single mammalian dynein molecules take 24–32 nm steps along MTs in the absence of load. In contrast, visualization of mammalian dynein bound nonspecifically to protein A-conjugated quantum dots revealed 8 nm center-of-mass steps ([74], Chapter 7). Using yeast dynein that was specifically covalently labeled with either an organic fluorophore or a quantum dot on the extreme N-terminus of the tail domain, Reck-Peterson *et al.* [55] reported a predominant 8 nm center of mass step size, as well as longer, backward, and frequent (~20%) sideways steps (Fig. 8.3B shows stepping behavior of dynein labeled on a single motor domain, which on average takes ~16 nm steps [55]). Earlier work performed

with bead-absorbed dynein also suggested that dynein could move laterally, although the step sizes could not be resolved in this work [80]. The studies of Reck-Peterson *et al.* [55] and Wang *et al.* [80] suggest that dynein has a considerable diffusional component to its step, a property that might aid dynein when navigating through the crowded subcellular environment. In fact, recent work examining the ability of dynein to navigate Tau-decorated MTs or intersecting MTs indicates that dynein can easily step around obstacles, while it is rare for kinesin to do so [5, 59]. Thus, some controversy still surrounds the dynein step size. Possible reasons for the different results reported include species-specific differences, differences in the method of attaching dynein to beads, or specific vs. nonspecific fluorescence labeling strategies.

Recent single-molecule fluorescence studies have also provided the first insights into dynein's "walking" mechanism, that is, how dynein's two-motor domains advance along MTs in a stepwise manner (Fig. 8.4). For myosin-V and kinesin-1 motors, one method used to address this question was to compare the stepping behavior of a single-motor domain to the stepping behavior of the motor's tail domain (center of mass). Such experiments demonstrated convincingly that both myosin-V and kinesin-1 step in a hand-over-hand fashion, with each motor domain alternately taking the leading position [86, 87] (Fig. 8.4). Similar experiments performed on dynein demonstrated that a single-motor domain takes steps that are twice as large as the centroid

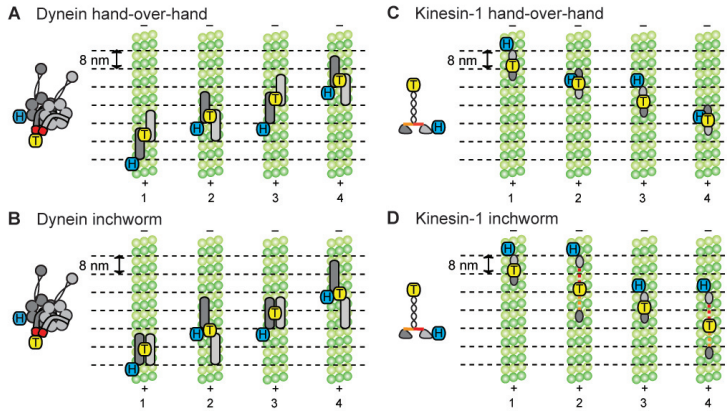

Figure 8.4. Possible stepping mechanisms for cytoplasmic dynein compared to kinesin-1. (A) Hand-over-hand stepping model for dynein. (B) Inchworm stepping model for dynein. (C) Hand-over-hand stepping model for kinesin-1. (D) Inchworm stepping model for kinesin-1. Because of the large size of the dynein molecule compared to kinesin-1 (drawn roughly to scale in relation to the MT), the existing stepping data for dynein are consistent with either a hand-over-hand or inchworm model. In contrast, due to the compact size of kinesin-1, the existing stepping data rules out an inchworm mechanism for kinesin-1. The kinesin-1 neck linker domain is shown in red and orange and is not long enough to accommodate a 16 nm step in the inchworm model (D).

position [55] (Fig. 8.3B). However, due to the large distance between the MTBD and dimerization site in the dynein molecule (possibly >40 nm), it is not yet possible to conclusively determine if dynein steps with each of its motor domains alternately taking the leading position or with a single-motor domain always leading, or some variation of these mechanisms (Fig. 8.4). Simultaneous observation of both motor domains during stepping will be needed to resolve this question.

8.3.3 Directionality of Cytoplasmic Dynein

Electron microscopy (EM) studies of an inner-arm axonemal dynein led to the first model for how dynein achieves minus-end-directed movement [2]. This work demonstrated that dynein's linker domain could adopt two different nucleotide-dependent conformations in relation to dynein's AAA+ ring [2], and later work confirmed that the same conformational change occurs in cytoplasmic dynein ([2, 57], Chapter 4). These experiments led to the hypothesis that if the dynein ring were in the same plane as the MT, dynein's observed directional bias could be achieved by an ATP-dependent movement of the linker domain toward the MT minus-end [2]. However, recent single-molecule and structural studies on dynein have led to a refined working model for dynein's MT minus-end-directed motility (described below) (Fig. 8.5).

Using optical tweezers, Gennerich *et al.* [11] demonstrated that dynein's affinity for MTs depends on the direction in which force is applied (Fig. 8.6D). In these experiments, single yeast dynein molecules moved processively along MTs with an applied external force in the absence of nucleotides, with less force required for minus-end-directed than for plus-end-directed stepping. Assuming that there is a leading and trailing head as dynein advances along the MT, a possible interpretation of this result is that intramolecular tension (that accumulates during the two-head-bound state) causes a minus-end-directed deflection of the MTBD-stalk domain of the trailing head leading to ATP-dependent detachment from the MT [11]. An asymmetric tension-sensing mechanism by the MTBD-stalk domain that favors rear-head detachment could thus keep the dynein heads out-of-phase during processive motion [11]. This mechanism could work in concert with a linker-driven powerstroke to bias dynein movement toward the MT minus-end.

Additional evidence that the direction in which the dynein stalks point is critical for determining directionality came from recent structural and functional studies [3]. In this work, mutations in dynein's long coiled coil stalk predicted to rotate dynein's AAA+ ring domains by 180° surprisingly showed that the mutant motors still generated minus-end-directed motion

(Fig. 8.5). According to the original model by Burgess *et al.* [2], such a rotation should have redirected the linker element displacement toward the MT plus-end, leading to plus-end-directed movement. The results of Carter *et al.* [3] suggest that the direction of dynein motion does not depend on the orientation of dynein's AAA+ ring domains relative to the MT axis. Rather, the data suggest that the conformational change of the linker element is directed parallel to a tilted stalk (extending from the AAA+ ring toward the MT minus-end), allowing the net displacement vector of the motor to remain parallel to the tilted stalk in the coiled coil mutant motors [3] (Fig. 8.5). In support of such a scenario, recent cryo-EM data reveal that the dynein stalk is tilted toward the MT minus-end when bound to MTs [3, 75] (see Chapters 5 and 6).

Dynein's directionality might also be subject to modification by dynein regulatory proteins; notably, the energy barrier difference for stepping in the forward and backward directions under unloaded conditions is low for dynein ($1.4k_BT$; [11]) as compared to the energy barrier difference measured for the MT plus-end-directed motor kinesin-1 ($5.4k_BT$; [50]). It is known that mammalian dynein-dynactin complexes can move bi-directionally on MTs, with plus-end-directed runs as long as 1 μm, although the majority of movements remain minus-end-directed [5, 58, 59]. However, these experiments were only performed with dynein-dynactin and not dynein alone, so it remains unclear whether the plus-end-directed motion of mammalian brain dynein-dynactin is due to dynactin or is a property of the dynein used in these studies. Yeast dynein or yeast dynein-dynactin does not display bi-directional properties (see Section 8.5.2) [22].

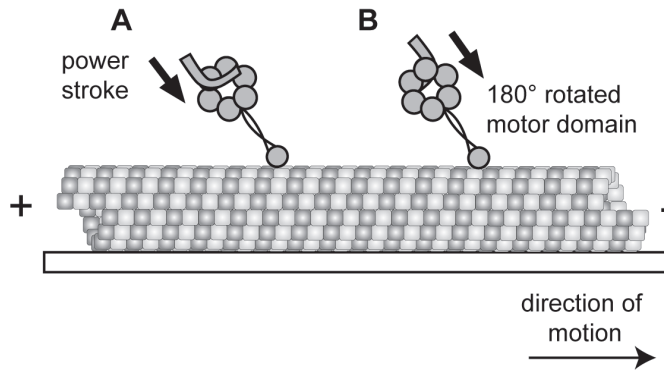

Figure 8.5 Model for dynein's power stroke. MT binding by dynein is followed by a displacement of the linker domain (power stroke) toward its MTBD and parallel to the tilted stalk (arrow), which generates movement toward the MT minus-end (A). The proposed model is consistent with MT minus-end-directed motion generated by a stalk mutant motor that has a predicated 180° rotated AAA+ ring domain (B) [3].

8.4 RESPONSE OF CYTOPLASMIC DYNEIN TO LOAD

The first evidence for the force-generating capabilities of isolated, individual cytoplasmic dynein molecules came from optical trapping studies on mammalian dynein purified from bovine brain tissue [38]. Mallik *et al.* [38] used optical tweezers to probe the nanoscale stepping and force production of single dynein molecules in the absence of the dynein cofactor dynactin. Single-beam optical tweezers, which consist of a tightly focused near-infrared laser beam, can be used to trap and hold a micrometer-sized polystyrene bead (Fig. 8.6A). When positioned over a coverslip-bound MT in the presence of ATP, a dynein-coated bead binds to and moves along the MT away from the trap center. The bead position can then be tracked with nanometer precision using a quadrant photodiode detector. Once the trapped bead is displaced from the trap center by dynein, a restoring force acts to pull the bead back toward the center of the trap (analogous to the restoring force of a Hookean spring). By observing dynein-powered bead motion under an increasing opposing force until movement slows and eventually ceases (Fig. 8.6B), Mallik *et al.* [38] found that individual dynein molecules nonspecifically absorbed to beads generate a maximal force of 1.1 pN under saturating ATP concentrations, and that the stall force linearly decreases with decreasing ATP concentration. Intriguingly, dynein's primary step size of 24–32 nm under unloaded conditions decreased to 8 nm under opposing loads of 1 pN, which lead the authors to conclude that dynein utilizes a gear mechanism.

Over the past few years, other groups have performed optical trapping studies on mammalian dynein [74, 79], the first recombinantly expressed full-length dynein [11], and truncated artificially dimerized dyneins [11]. Several controversies have arisen in the data leading to an ongoing discussion on dynein's stepping and stalling behavior. Toba *et al.* [74] demonstrated that porcine brain dynein nonspecifically absorbed to protein A-coated beads takes load-invariant 8 nm steps against an ATP-insensitive maximal force of 7 pN (Chapter 7), which is surprisingly similar to the stepping and stalling behavior of the MT plus-end-directed motor kinesin-1 [71] and is in contrast to the earlier work on bovine dynein [38]. The motion of single recombinant *S. cerevisiae* dynein molecules attached specifically by their tail domains to beads also was found to cease under an opposing load of ~7 pN at both saturating and limiting ATP concentrations, in contrast to the earlier report by Mallik *et al.* [38] but in agreement with Toba *et al.* [74]. Yeast dynein advances predominantly with 8 nm steps but also takes a fraction of larger (12–24 nm) force-dependent steps (Fig. 8.6C), resembling findings by both Toba *et al.* [74] and Mallik *et al.* [38]. Notably, while mammalian dynein and kinesin-1 dissociate within seconds from the MT at stall loads [38, 74], yeast dynein

frequently remains bound tenaciously to the MT for minutes before dissociating [11] (Fig. 8.6B). Because it has been estimated that only 2–3 dynein dimers [39] are present at sites where cortical yeast dynein pulls the large elongating spindle into the daughter cell during cell division, this property of yeast dynein may be specifically tailored for this role, the only known function for dynein in yeast cells (Chapter 15).

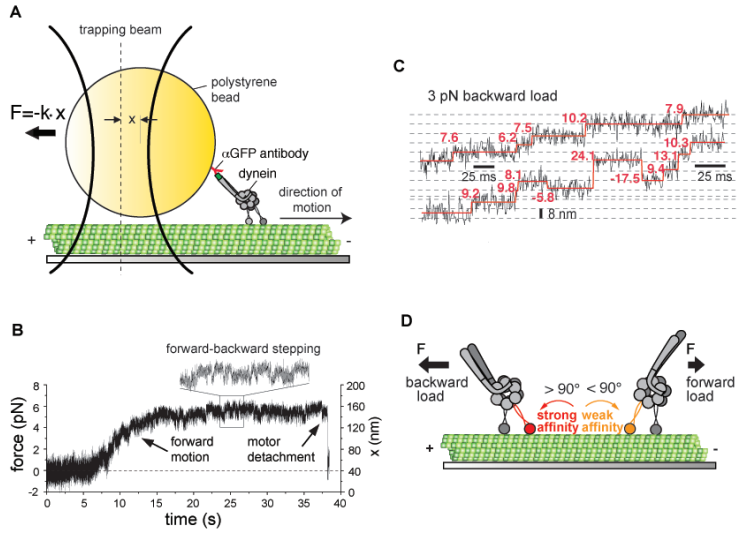

Figure 8.6 Dissecting dynein function using optical tweezers. (A) Schematic representation of the optical trapping assay (not to scale). (B) Force generation and stalling of a single artificially dimerized (with GST) yeast dynein molecule at 1 mM ATP in a fixed optical trap (non-feedback mode) (adapted from Fig. 2 of Gennerich and Reck-Peterson [12]). The inserted trace segment, which shows an example of continuous forward-backward stepping, corresponds to the part of the stalling trace indicated by the rectangular box. (C) Example optical trapping records of processive forward stepping of a single full-length dynein molecule against a constant load of 3 pN (force-feedback mode) (adapted from Fig. 4B of Gennerich *et al.* [11]) showing consecutive ~8 nm steps and a single 24 nm step. The raw data are shown in black and the steps detected by a step finding program [24] in red (trap stiffness: $k = 0.03$ pN/nm). (D) Model for dynein's MT-affinity regulation by external force (or intramolecular strain, respectively). The key feature of the proposed mechanism is a tension-sensing mechanism by dynein's MTBD. In this model, forward deflection of the stalk (induced by external forward load or intramolecular strain provided by a power stroke; schematic right) weakens the binding affinity of the MTBD in the rear head (indicated by the orange-colored stalk). This mechanism favors rear head detachment and thus helps to keep the dynein heads out-of-phase during continuous movement toward the MT minus-end. Backward load potentially increases the MT-binding affinity of the MTBD in the front head (caused by a load-induced backward deflection of the stalk; indicated by the red-colored stalk in the left schematic), which could explain the large external loads required to induce backward stepping.

While much clarifying work is needed, a new optical trapping study on porcine dynein [79] adds to the existing controversy. Using a three-bead optical trapping assay, Walter *et al.* [79] demonstrate that mammalian brain dynein takes regular 8 nm steps under opposing forces of up to ~5 pN, results which are largely in agreement with the report by Toba *et al.* [74]. However, Walter *et al.* [79] also find that dynein's force generation decreases to 1 pN at 50 μM ATP, a result that is reminiscent of a key finding reported by Mallik *et al.* [38] but in contrast to the findings by Toba *et al.* [74] and Gennerich *et al.* [11]. Collectively, further work is required to resolve the discrepancies in the reported dynein stepping behavior under load and the ATP-dependency of dynein's force generation, with particular attention paid to the biochemical assay conditions, dynein cofactor stoichiometry, and the dynein-bead attachment method.

Force-clamp optical tweezers experiments (a technique that allows studying motor stepping under an average constant force) combined with hypothesis-driven structure function studies have provided the first insights into the molecular mechanism underlying dynein stalling [11]. Motor stalling occurs when the applied force load approaches a value at which the likelihood for a forward step equals the likelihood for a backward step. This force-induced change in the stepping behavior often results in continuous forward-backward stepping [11] (Fig. 8.6B, inset). Applied forces can potentially decrease the probability for a forward step in several not mutually exclusive ways. Force could slow down force-sensitive mechanical transitions such as displacement-generating and large-scale conformational changes, which could diminish the likelihood for a successful forward step. In addition, load could decrease the likelihood that dynein's trailing head passes the leading head by imposing steric constraints as a result of a force-induced modification of the dynein geometry. Furthermore, the external force could reverse a forward step (rather than preventing it) by detaching the newly MT-bound front head and then pulling it backward past its partner head. However, while an effect on force-sensitive transitions remains possible, the recent study by Gennerich *et al.* [11] provides hints that dynein's forward step is force insensitive and suggests that dynein stalling occurs due to a force-induced unbinding of dynein's front head.

If the force necessary to unbind a dynein head from its track determines the dynein stall force, an applied superstall force (an opposing load that exceeds the stall force) should cause dynein to walk backwards. In agreement with this prediction, a constant 10 pN superstall load applied to yeast dynein (following motor stalling at 7 pN) induces processive MT plus-end-directed stepping in the presence or absence of ATP [11]. This result demonstrates that

force alone can cause repetitive MT detachment-attachment cycles of dynein's motor domains. Force-induced nucleotide independent stepping has also been recently reported for kinein-1 [88] and myosin-V [8], suggesting a general mechanistic feature among processive cytoskeletal motors. Interestingly, unlike myosin-V, dynein can also be induced to step in the forward direction (by a substall force) in the absence of nucleotides [11]. The ability of dynein to step both forward and backward in an ATP-independent, but force-dependent manner, raises the intriguing possibility that an "unsynchronized" ("out-of-phase") or "inactive" dynein motor within an assembly of multiple MT- and cargo-bound dyneins could passively follow the stepping imposed by the active, force-generating subset of motors without dissociating from its track. Such a property could be important for synchronizing multiple dynein motors acting on the same cargo, such as during long-distance organelle transport, the dynein-based cortical sliding of MTs during cell division, or the advancement of MTs during the outgrowth of axons [15].

Structure-function and optical trapping studies also demonstrate that dynein's linker elements provide the necessary head-head spacing that allows dynein to take consecutive forward-backward steps at stall load and that the force necessary to cease dynein motion is sensitive to the length of dynein's linker elements [11]. Decreasing the head-to-head separation (or reach) of the dynein dimer by truncating dynein's linker elements results in a reduced stall force, while the force necessary to unbind a dynein head remains unchanged as compared to wild-type dynein [11]. In addition, inserting artificial linker elements in the truncated motors results in a stall force increase. This result suggests that a longer linker element increases the likelihood of the trailing head being able to pass its partner head at a given load by minimizing steric constraints. Collectively, these results suggest that dynein's maximal force generation is limited by the motor's MT-binding strength under backward load, and that dynein's linker elements provide the necessary head-head spacing that is prerequisite for dynein's ability to take forward-backward steps during motor stalling (Fig. 8.6B).

8.5 REGULATION OF CYTOPLASMIC DYNEIN MOTILITY

We are still just beginning to understand how cytoplasmic dynein is regulated [21]. Given that at least 39 polypeptides and 19 different genes are required for mammalian dynein function (at least 29 polypeptides and 11 genes in yeast), and that dynein can bind up to eight molecules of ATP/ADP per dimer, it is clear that there are many possible points of regulation. Here we will focus on the two points of regulation that have been shown experimentally

to affect motile behavior: dynein's multiple ATP-binding AAA+ domains and some of dynein's associated regulatory cofactors, dynactin, LIS1, and NudE (see Chapter 2).

8.5.1 AAA+ Domains

Dynein is an atypical member of the AAA+ family of ATPases [51]. Unlike most other AAA+ ATPases, many of which are composed of six copies of identical AAA+ subunits that oligomerize into hexamers, dynein's six AAA+ domains are connected as a single polypeptide, with each domain encoding a slightly different AAA+ sequence. Early experiments demonstrated that in the presence of vanadate and ATP, UV irradiation resulted in a photo-cleavage event at AAA1 that inactivated dynein's ATPase activity, providing the first evidence that AAA1 was likely the primary site of ATP hydrolysis in dynein [13, 52]. When recombinant protein became available, this result was confirmed and extended to the analysis of the role of each AAA+ domain for ATPase activity, motility, and *in vivo* function [4, 28, 54, 67] (Table 8.1, see also Section 3.3).

8.5.1.1 AAA1

A point mutation expected to block nucleotide binding at AAA1 inhibits motility driven by monomeric dynein in a MT-gliding assay [28]. A similar mutation in a two-headed dimeric dynein results in a nonmotile motor in single-molecule TIRF assays (Reck-Peterson and Vale, unpublished data).

8.5.1.2 AAA2, AAA4

Mutations expected to block nucleotide binding at AAA2 and AAA4 have only subtle effects on MT motility driven by monomeric dynein [28]. However, mutations expected to block ATP hydrolysis at AAA4 increase the processivity of dimeric dynein [4]. While proteins that might regulate ATPase activity at AAA4 have not been identified, this result raises the possibility that stimulating ATP hydrolysis at AAA4 could lead to processive run termination.

8.5.1.3 AAA3

Mutations predicted to block nucleotide binding at AAA3 result in dramatically decreased velocity of monomeric dynein in MT-sliding assays [28]. Interestingly, in single-molecule assays an ATP hydrolysis AAA3 mutant

is as processive as wild-type dynein, but moves 20 times slower [4]. This reduced velocity is due to both a much higher MT-binding affinity as well as a decrease in MT-stimulated ATPase activity. The effect on ATPase activity is most likely due to allosteric communication between AAA1 (the principal site of ATP hydrolysis) and AAA3.

Table 8.1 AAA+ Domain Mutation Effects on Dynein Motility

AAA+ domain	MT-stimulated ATPase	MT-gliding velocity	Single-molecule velocity	Single-molecule run length	Single-molecule stall force	*In vivo* function
Wild-type	100%[28]	100%[28]	100%[4]	100%[4]	100%[4]	100%[4, 54]
AAA1 A	4% [28]	0%[28]		–	–	30%[54]
AAA1 B	–	–	0%	0%	–	36%[54]
AAA2 A	25%[28]	75%[28]	–	–	–	95%[54]
AAA2 B	–	–	–	–	–	–
AAA3 A	5%[28]	4%[28]	–	–	–	32%[54]
AAA3 B	–	–	7%[4]	89%[4]	58%[4]	29%[4, 54]
AAA4 A	4%[28]	42%[28]	–	–	–	99%[54]
AAA4 B	–	–	86%[4]	229%[4]	82%[4]	100%[4, 54]

All numbers are listed as a percent of wild-type activity, with wild-type activity being 100%. "A" and "B" represent Walker-A and Walker-B mutations in each AAA+ domain. Walker-A mutations are expected to block ATP binding and Walker-B mutations are expected to block ATP hydrolysis. MT-stimulated ATPase activity and MT-gliding velocities were measured with monomeric *Dictyostelium* motors [28]. Single-molecule velocity, run lengths (processivity), and stall forces were measured with dimeric *S. cerevisiae* motors [4]. *In vivo* function was measured in *S. cerevisiae* as the ability to segregate nuclei to daughter cells, a process that requires dynein [4, 54].

Despite the fact that mutations in AAA+ domains 1–4 all have some phenotype either *in vitro* or *in vivo*, the number of ATP molecules hydrolyzed per step remains uncertain. Analysis of the dwell times between steps at rate-limiting ATP concentrations should provide this information. However, analysis of stepping experiments performed for either brain or yeast dynein (under unloaded conditions) suggests that only one ATP is used per step, based on the fact that the dwell time data is best fit by a single exponential function [38, 55, 74]. In addition, in yeast, the ATPase rate (16 Pi/s/dimer)

and step size (8 nm with an 80% probability of taking a forward step) suggest that only one ATP is used per step given the measured velocity (~100 nm/s) in the presence of saturating ATP concentrations [4, 55]. Thus, the role of each AAA+ domain in the dynein mechanism remains unclear. Possibilities that remain to be tested experimentally include determining whether some AAA+ domains preferentially bind ADP, hydrolyze ATP at a much lower rate than AAA1, or have a much higher affinity for nucleotide compared to AAA1.

8.5.2 Dynein Cofactors

8.5.2.1 Dynactin

Dynactin was originally identified as an activator of dynein-mediated vesicle transport [14, 62] and is required for nearly all dynein functions in cells. Mammalian dynactin is approximately 1.2 MDa and is composed of at least 23 different polypeptides, while the yeast complex contains at least 17 polypeptides [44, 63]. In a bead-based *in vitro* motility assay, dynein-coated beads in the presence of dynactin move greater distances than dynein-coated beads in the absence of dynactin, indicating that dynactin acts as a dynein processivity factor [26]. It was hypothesized that this effect may be due to the MT-binding domains (MTBDs) in the $p150^{Glued}$ dynactin subunit acting as an additional MT tether, capable of keeping dynein-dynactin molecules attached to MTs even if both dynein motor domains detached [26, 83].

The recent development of a source of recombinant dynactin [22] has now allowed the mechanism of dynactin's processivity effect to be dissected. Using purified recombinant *S. cerevisiae* dynactin, Kardon *et al.* [22] confirmed that dynactin is a dynein processivity factor using a direct single-molecule approach. In these studies a small organic fluorophore was covalently linked to the dynactin $p150^{Glued}$ (Nip100 in yeast) subunit and single dynein-dynactin complexes could be observed moving processively along MTs using TIRF microscopy. Mutational analysis demonstrated that the MTBD of yeast dynactin was not required for processivity enhancement, while other structural features of the dynactin complex were [22]. Because both dynein and dynactin are composed of multiple dimeric subunits that are necessary for the dynein-dynactin interaction, processivity enhancement could be achieved by dynactin-mediated multimerization of dynein dimers. Photobleaching studies were used to rule out this mechanism [22]. Other possible mechanisms for processivity enhancement remain to be tested. For

example, King *et al.* [26] found that dynein-dynactin had a higher affinity for MTs than dynein alone. These experiments have not been repeated using the recombinant dynactin mutants lacking the MTBD. It is possible that dynactin increases dynein's MT-binding affinity allosterically without binding to MTs on its own. Another possibility that could be tested using high-precision analysis of dynein's stepping behavior in the presence of dynactin is that dynactin could alter dynein's stepping behavior and/or head-to-head coordination. Because dynein is able to take frequent sideways, backwards, and large forward steps that could potentially cause a premature termination of a processive run, it is possible that a dynein-associated factor that "constrained" dynein to take more regular 8 nm forward steps would lead to a more efficient and processive motor. Dynein stepping experiments in the presence or absence of dynactin have not yet been performed to test this possible mechanism for dynactin's processivity effect on dynein.

Interestingly, recent *in vivo* studies in *Drosophila* S2 cells and yeast suggest that dynactin's MTBD is required in cellular contexts in which dynein is expected to be moving against higher loads [25, 43]. The behavior of dynein-dynactin has not yet been examined in optical tweezers experiments *in vitro*, but such experiments will be able to directly test the hypothesis that dynactin's MTBD allows dynein to remain MT bound for longer times under loads and, possibly, to pull against higher loads. It is possible that dynactin has two separable functions, to increase dynein processivity (which does not require the dynactin MTBD) and to increase the ability of dynein to work against load (which requires the dynactin MTBD); additional analysis of mutants in single-molecule assays in both loaded and unloaded conditions will be required to understand these properties of dynactin at a mechanistic level.

The directionality of dynein-dynactin motor complexes has also been investigated and is controversial. Using purified murine brain dynein-dynactin, Ross *et al.* [58] reported that dynein-dynactin complexes undergo long (>1000 nm) movements toward both the plus- and minus-ends of MTs. In contrast, high-precision experiments using the recombinant yeast complex found that the majority of dynein-dynactin runs advanced toward the minus-end of MTs even at the level of single steps (only 2% of plus-end-directed segments were >24 nm [22]). The discrepancy in the reported behavior between these two dynein-dynactin complexes could be species-specific, due to differences in the assay conditions, or variability in the stoichiometry of associated subunits or cofactors; further work will be necessary to resolve this.

8.5.2.2 LIS1 and NudE

The *LIS1* gene was originally identified by positional cloning as a gene linked to classical lissencephaly, a brain developmental disease characterized by defects in cortical organization [6, 56]. *LIS1* was later linked to the dynein pathway when it was found that mutations in a filamentous fungus (*Aspergillus nidulans*) homologue of the gene caused a nuclear migration phenotype that resembled the defect caused by mutations in the cytoplasmic dynein heavy chain gene, *nudA* [84]. Similarly, ro-11/*nudE* was first identified in another filamentous fungus (*Neurospora crassa*) as a gene that caused a dynein-like nuclear migration phenotype when mutated [7, 42], and was further tied to the dynein pathway by experiments demonstrating that *nudE* and *nudF*/*LIS1* interact both genetically and biochemically [7]. Shortly thereafter a mammalian homologue of *nudE* was identified and named NUDEL (*nudE*-like) [48, 61]. Additional names and homologues of NUDEL include NDE1, NDEL1, and NUDE; here we will refer to *nudE* generically as NudE and *nudF*/*LIS1* as LIS1. It has since been shown that LIS1 and NudE form a stable heterotetramer that makes multiple contacts with the dynein complex [72, 73].

While it is clear that both LIS1 and NudE are required for dynein function in many organisms [21], their role in dynein motility is only beginning to be understood. A recent study by McKenney *et al.* [41] demonstrates that while NudE has inhibitory effects on dynein motion, LIS1 alone and LIS1/NudE together increase the stalling time of single dynein molecules. Biochemical and biophysical experiments suggest that NudE stabilizes the LIS1-dynein interaction and that the dynein-LIS1-NudE motor complex has increased processivity and significantly increased capabilities to remain MT-bound under load. Furthermore, this enhancement of detachment kinetics under load by LIS1 and NudE was shown to augment multiple motor-driven transport [41]. The authors suggest that these properties of LIS1 and NudE could allow dynein to act as a persistent force generator for functions that require the motor to work against higher loads, such as nuclear and MT organizing center movement [41]. Another study has shown that LIS1 is an inhibitor of dynein motility [85]. In this work, MT-gliding assays demonstrated that brain cytoplasmic dynein-driven MT gliding is almost completely inhibited in the presence of LIS1 and that this inhibition can be overcome by adding NudE. Intriguingly LIS1 and NudE have been shown to be important for dynein MT plus-end localization (reviewed in [21]), which in fungi is a prerequisite for localization to the plasma membrane where dynein functions to pull on nuclei-attached MTs [36, 37, 64]. Dynein's stable association with MT

plus-ends suggests that the motor is kept in an inactive state; the results of Yamada *et al.* [85] raise the possibility that LIS1 could be responsible for this activity.

8.6 *IN VIVO* STUDIES OF DYNEIN MOTILITY

An ultimate goal of the field is to understand how molecular motors move and transport cargoes in cells (reviewed in [19]). Experiments are only beginning to address this question, limited largely by the technical difficulties of tracking motors with sufficient spatial precision and temporal resolution at cellular ATP concentrations, and labeling motors directly *in vivo*. Thus far, the general method used to track dynein motors in cells has been to monitor a dynein cargo that is either fluorescently labeled for the use of epi-fluorescence or TIRF microscopy or has optical properties that allow the use of light-scattering-based techniques. In these experiments, movements away from the cell center are presumed to be kinesin-driven and movements toward the cell center dynein-driven. Several reports have suggested that the primary step size in both directions is 8 nm [32, 33, 81, 82], while others have seen a more variable step size for dynein-based transport [46, 47, 68], more consistent with the *in vitro* studies of Mallik *et al.* [38], Reck-Peterson *et al.* [55], and Gennerich *et al.* [11].

The interpretation of *in vivo* experiments is complicated due to the uncertainty about the number of motors involved in the observed cargo displacements, and the fact that multiple motors can generate fractional cargo steps [34]. However, using stall force measurement as an indirect measure of the number of contributing motors, Sims and Xie [68] revealed a strong asymmetry in step-size distributions for presumed transport by single kinesin and dynein molecules. While outward movements occurred with 8 nm steps, inward-generated cargo displacements revealed a predominant step size of 8 nm but also longer steps of 12–24 nm, consistent with previously reported *in vitro* observations [11, 55]. Thus, rather than resolving current discrepancies among *in vitro* studies, *in vivo* experiments seem to support both types of stepping modes observed *in vitro* (invariable and variable stepping behaviors, respectively) and add to the existing controversies. Nevertheless, the similarities among *in vivo* and *in vitro* observations across species (e.g., variable step sizes of dynein in human lung cancer cells and single yeast dynein *in vitro*) [11, 47, 55, 68] indicate that the discrepancies among reported step sizes are not necessarily attributable to species-specific differences, as often assumed.

The magnitude of forces that dynein motors generate in living cells is also a point of continuing debate. The *in vivo* dynein stall force has been estimated to be 1.1 pN based on the stalling behavior of endogenous cargo moving toward the center of the cell [16, 69], which is in agreement with *in vitro* reports by Mallik *et al.* [38]. However, other studies suggest a maximal *in vivo* force generation of dynein in the range of 3–5 pN [66, 68]. Single-molecule stall forces are of particular interest when modeling bidirectional organelle transport, which is characterized by frequent direction reversals. Notably, a recent theoretical study demonstrated that a "tug-of-war" between kinesin and dynein motors (assuming the 1.1 pN *in vitro* stall force observed by Mallik *et al.* [38]) could explain the commonly observed switching between fast plus-end-directed and fast minus-end-directed motion [45], and there is *in vivo* experimental support for this idea as well [10, 69]. As the results among *in vivo* force measurements differ significantly, more work will be required to exclude cell type variations and uncertainties in data acquisition and analysis, with particular attention to the calibration of the optical tweezers setup for *in vivo* experiments.

8.7 CONCLUSIONS AND FUTURE DIRECTIONS

Clearly the next few years promise to be an exciting time for the dynein field. The pace of research in the field has increased rapidly with the advent of recombinant systems for protein expression and the application of single-molecule approaches to understand the dynein motility mechanism. In addition to resolving the controversies surrounding the dynein stepping mechanism and response to force, a number of other areas related to dynein regulation remain to be dissected. The mechanism of processivity enhancement by dynactin still awaits a molecular mechanism, as do the possible roles for LIS1 in either dynein motor activity inhibition or the ability to induce a load-resistant, strongly MT-bound state. While there is evidence that both the dynein HC and some of its associated subunits are phosphorylated [31, 60], the possible role of phosphorylation in regulating cytoplasmic dynein motility has not been addressed. Similarly, while dynein subunit heterogeneity has been documented [17, 35, 70], whether this results in motor populations with distinct motile properties has not yet been investigated. Further advances in recombinant approaches as well as more detailed structural information about the dynein HC, associated subunits, and cofactors will be important for continuing to refine our understanding of the dynein stepping mechanism.

Acknowledgements

The authors thank Andres Leschziner for comments on the manuscript and Weihong Qiu for help in generating the figures.

References

1. Bingham, J. B., King, S. J. and Schroer, T. A. (1998). Purification of dynactin and dynein from brain tissue. *Methods Enzymol.*, **298**, pp. 171–184.
2. Burgess, S. A., Walker, M. L., Sakakibara, H., Knight, P. J. and Oiwa, K. (2003). Dynein structure and power stroke. *Nature*, **421**(6924), pp. 715–718.
3. Carter, A. P., Garbarino, J. E. Wilson-Kubalek, E. M., Shipley, W. E., Cho, C., Milligan, R. A., Vale, R. D. and Gibbons, I. R. (2008). Structure and functional role of dynein's microtubule-binding domain. *Science*, **322**(5908), pp. 1691–1695.
4. Cho, C., Reck-Peterson, S. L. and Vale, R. D. (2008). Regulatory ATPase sites of cytoplasmic dynein affect processivity and force generation. *J. Biol Chem.,* **283**(38), pp. 25839–25845.
5. Dixit, R., Ross, J. L., Goldman, Y. E. and Holzbaur, E. L. (2008). Differential regulation of dynein and kinesin motor proteins by tau. *Science*, **319**(5866), pp. 1086–1089.
6. Dobyns, W. B., Reiner, O., Carrozzo, R. and Ledbetter, D. H. (1993). Lissencephaly. A human brain malformation associated with deletion of the LIS1 gene located at chromosome 17p13. *JAMA*, **270**(23), pp. 2838–2342.
7. Efimov, V. P. and Morris, N. R. (2000). The LIS1-related NUDF protein of *Aspergillus nidulans* interacts with the coiled-coil domain of the NUDE/RO11 protein. *J. Cell Biol.*, **150**(3), pp. 681–688.
8. Gebhardt, J. C., Clemen, A. E., Jaud, J. and Rief, M. (2006). Myosin-V is a mechanical ratchet. *Proc. Natl. Acad. Sci. USA*, **103**(23), pp. 8680–8685.
9. Gee, M. A., Heuser, J. E. and Vallee, R. B. (1997). An extended microtubule-binding structure within the dynein motor domain. *Nature*, **390**(6660), pp. 636–639.
10. Gennerich, A. and Schild, D. (2006). Finite-particle tracking reveals submicroscopic-size changes of mitochondria during transport in mitral cell dendrites. *Phys. Biol.,* **3**(1), pp. 45–53.
11. Gennerich, A., Carter, A. P., Reck-Peterson, S. L. and Vale, R. D. (2007). Force-induced bidirectional stepping of cytoplasmic dynein. *Cell*, **131**(5), pp. 952–965.
12. Gennerich, A. and Reck-Peterson, S. L. (2010) Probing the force generation and stepping behavior of cytoplasmic dynein, in Single Molecule Techniques, Methods in Molecular Biology Series, Wuite, G. and Peterman, E., eds. (Humana Press). In press.
13. Gibbons, I. R., Lee-Eiford, A., Mocz, G., Phillipson, C. A., Tang, W. J. and Gibbons, B. H. (1987). Photosensitized cleavage of dynein heavy chains. Cleavage at the "V1 site" by irradiation at 365 nm in the presence of ATP and vanadate. *J. Biol. Chem.*, **262**(6), pp. 2780–2786.

14. Gill, S. R., Schroer, T. A., Szilak, I., Steuer, E. R., Sheetz, M. P. and Cleveland, D. W. (1991). Dynactin, a conserved, ubiquitously expressed component of an activator of vesicle motility mediated by cytoplasmic dynein. *J. Cell Biol.*, **115**(6), pp. 1639–1650.

15. Grabham, P. W., Seale, G. E., Bennecib, M., Goldberg, D. J. and Vallee, R. B. (2007). Cytoplasmic dynein and LIS1 are required for microtubule advance during growth cone remodeling and fast axonal outgrowth. *J. Neurosci.,* **27**(21), pp. 5823–5834.

16. Gross, S. P., Welte, M. A., Block, S. M. and Wieschaus, E. F. (2000). Dynein-mediated cargo transport *in vivo*. A switch controls travel distance. *J. Cell Biol.*, **148**(5), pp. 945–956.

17. Ha, J., Lo, K. W., Myers, K. R., Carr, T. M., Humsi, M. K., Rasoul, B. A., Segal, R. A. and Pfister, K. K. (2008). A neuron-specific cytoplasmic dynein isoform preferentially transports TrkB signaling endosomes. *J. Cell Biol.*, **181**(6), pp. 1027–1039.

18. Hays, T. S., Porter, M. E., McGrail, M., Grissom, P., Gosch, P., Fuller, M. T. and McIntosh, J. R. (1994). A cytoplasmic dynein motor in *Drosophila*: identification and localization during embryogenesis. *J. Cell Sci.*, **107** (6), pp. 1557–1569.

19. Holzbaur, E. L. and Goldman, Y. E. (2010). Coordination of molecular motors: from in vitro assays to intracellular dynamics. *Curr. Opin. Cell Biol.*, **22**(1), pp. 4–13.

20. Hook, P., Mikami, A., Shafer, B., Chait, B. T., Rosenfeld, S. S. and Vallee, R. B. (2005). Long range allosteric control of cytoplasmic dynein ATPase activity by the stalk and C-terminal domains. *J. Biol. Chem.*, **280**(38), pp. 33045–33054.

21. Kardon, J. R. and Vale, R. D. (2009). Regulators of the cytoplasmic dynein motor. *Nat. Rev. Mol. Cell. Biol.,* **10**(12), pp. 854–865.

22. Kardon, J. R., Reck-Peterson, S. L. and Vale, R. D. (2009). Regulation of the processivity and intracellular localization of *Saccharomyces cerevisiae* dynein by dynactin. *Proc. Natl. Acad. Sci. USA*, **106**(14), pp. 5669–5674.

23. Karki, S. and Holzbaur, E. L. (1999). Cytoplasmic dynein and dynactin in cell division and intracellular transport. *Curr. Opin. Cell Biol.*, **11**(1), pp. 45–53.

24. Kerssemakers, J. W., Munteanu, E. L., Laan, L., Noetzel, T. L., Janson, M. E. and Dogterom, M. (2006). Assembly dynamics of microtubules at molecular resolution. *Nature*, **442**(7103), pp. 709–712.

25. Kim, H., Ling, S. C., Rogers, G. C., Kural, C., Selvin, P. R., Rogers, S. L. and Gelfand, V. I. (2007). Microtubule binding by dynactin is required for microtubule organization but not cargo transport. *J. Cell Biol.*, **176**(5), pp. 641–651.

26. King, S. J. and Schroer, T. A. (2000). Dynactin increases the processivity of the cytoplasmic dynein motor. *Nat. Cell Biol.*, **2**(1), pp. 20–24.

27. Kon, T., Mogami, T., Ohkura, R., Nishiura, M. and Sutoh, K. (2005). ATP hydrolysis cycle-dependent tail motions in cytoplasmic dynein. *Nat. Struct. Mol. Biol.*, **12**(6), pp. 513–519.

28. Kon, T., Nishiura, M., Ohkura, R., Toyoshima, Y. Y. and Sutoh, K. (2004). Distinct functions of nucleotide-binding/hydrolysis sites in the four AAA modules of cytoplasmic dynein. *Biochemistry*, **43**(35), pp. 11266–11274.

29. Koonce, M. P. and Samso, M. (1996). Overexpression of cytoplasmic dynein's globular head causes a collapse of the interphase microtubule network in *Dictyostelium*. *Mol. Biol. Cell*, **7**(6), pp. 935–948.

30. Kumar, S., Lee, I. H. and Plamann, M. (2000). Two approaches to isolate cytoplasmic dynein ATPase from *Neurospora crassa*. *Biochimie*, **82**(3), pp. 229–236.

31. Kumar, S., Lee, I. H. and Plamann, M. (2000). Cytoplasmic dynein ATPase activity is regulated by dynactin-dependent phosphorylation. *J. Biol. Chem.*, **275**(41), pp. 31798–31804.

32. Kural, C., Kim, H., Syed, S., Goshima, G., Gelfand, V. I. and Selvin, P. R. (2005). Kinesin and dynein move a peroxisome *in vivo*: a tug-of-war or coordinated movement? *Science*, **308**(5727), pp. 1469–1472.

33. Kural, C., Serpinskaya, A. S., Chou, Y. H., Goldman, R. D., Gelfand, V. I. and Selvin, P. R. (2007). Tracking melanosomes inside a cell to study molecular motors and their interaction. *Proc. Natl. Acad. Sci. USA*, **104**(13), pp. 5378–5382.

34. Leduc, C., Ruhnow, F., Howard, J. and Diez, S. (2007). Detection of fractional steps in cargo movement by the collective operation of kinesin-1 motors. *Proc. Natl. Acad. Sci. USA*, **104**(26), pp. 10847–10852.

35. Lee, I. H., Kumar, S. and Plamann, M. (2001). Null mutants of the *Neurospora* actin-related protein 1 pointed-end complex show distinct phenotypes. *Mol. Biol. Cell*, **12**(7), pp. 2195–2206.

36. Lee, W. L., Oberle, J. R. and Cooper, J. A. (2003). The role of the lissencephaly protein Pac1 during nuclear migration in budding yeast. *J. Cell Biol.*, **160**(3), pp. 355–364.

37. Li, J., Lee, W. L. and Cooper, J. A. (2005). NudEL targets dynein to microtubule ends through LIS1. *Nat. Cell Biol.*, **7**(7), pp. 686–690.

38. Mallik, R., Carter, B. C., Lex, S. A., King, S. J. and Gross, S. P. (2004). Cytoplasmic dynein functions as a gear in response to load. *Nature*, **427**(6975), pp. 649–652.

39. Markus, S. M., Punch, J. J. and Lee, W. L. (2009). Motor- and tail-dependent targeting of dynein to microtubule plus ends and the cell cortex. *Curr. Biol.,* **19**(3), pp. 196–205.

40. Mazumdar, M., Mikami, A., Gee, M. A. and Vallee, R. B. (1996). *In vitro* motility from recombinant dynein heavy chain. *Proc. Natl. Acad. Sci. USA*, **93**(13), pp. 6552–6556.

41. McKenney, R. J., Vershinin, M., Kunwar, A., Valee, R. B. and Gross, S. P. (2010). LIS1 and NudE induce a persistent dynein force-producing state. *Cell*, **141**(2), pp. 304–314.

42. Minke, P. F., Lee, I. H., Tinsley, J. H., Bruno, K. S. and Plamann, M. (1999). *Neurospora crassa* ro-10 and ro-11 genes encode novel proteins required for nuclear distribution. *Mol. Microbiol.,* **32**(5), pp. 1065–1076.

43. Moore, J. K., Sept, D. and Cooper, J. A. (2009). Neurodegeneration mutations in dynactin impair dynein-dependent nuclear migration. *Proc. Natl. Acad. Sci. USA*, **106**(13), pp. 5147–5152.

44. Moore, J. K., Li, J. and Cooper, J. A. (2008). Dynactin function in mitotic spindle positioning. *Traffic*, **9**(4), pp. 510–527.

45. Muller, M. J., Klumpp, S. and Lipowsky, R. (2008). Tug-of-war as a cooperative mechanism for bidirectional cargo transport by molecular motors. *Proc. Natl. Acad. Sci. USA*, **105**(12), pp. 4609–4614.

46. Nan, X., Sims, P. A., Chen, P. and Xie, X. S. (2005). Observation of individual microtubule motor steps in living cells with endocytosed quantum dots. *J. Phys. Chem. B*, **109**(51), pp. 24220–24224.

47. Nan, X., Sims, P. A. and Xie, X. S. (2008). Organelle tracking in a living cell with microsecond time resolution and nanometer spatial precision. *ChemPhysChem,* **9**(5), pp. 707–712.

48. Niethammer, M., Smith, D. S., Ayala, R., Peng, J., Ko, J., Lee, M. S., Morabito, M. and Tsai, L. H. (2000). NUDEL is a novel Cdk5 substrate that associates with LIS1 and cytoplasmic dynein. *Neuron*, **28**(3), pp. 697–711.

49. Nishiura, M., Kon, T., Shiroguchi, K., Ohkura, R., Shima, T., Toyoshima, Y. Y. and Sutoh, K. (2004). A single-headed recombinant fragment of *Dictyostelium* cytoplasmic dynein can drive the robust sliding of microtubules. *J. Biol. Chem.*, **279**(22), pp. 22799–22802.

50. Nishiyama, M., Higuchi, H. and Yanagida, T. (2002). Chemomechanical coupling of the forward and backward steps of single kinesin molecules. *Nat. Cell Biol.*, **4**(10), pp. 790–797.

51. Ogura, T. and Wilkinson, A. J. (2001). AAA+ superfamily ATPases: common structure–diverse function. *Genes Cells*, **6**(7), pp. 575–597.

52. Paschal, B. M., Shpetner, H. S. and Vallee, R. B. (1987). MAP 1C is a microtubule-activated ATPase which translocates microtubules *in vitro* and has dynein-like properties. *J. Cell Biol.*, **105**(3), pp. 1273–1282.

53. Pfister, K. K., Shah, P. R., Hummerich, H., Russ, A., Cotton, J., Annuar, A. A., King, S. M. and Fisher, E. M. (2006). Genetic analysis of the cytoplasmic dynein subunit families. *PLoS Genet.*, **2**(1), pp. e1.

54. Reck-Peterson, S. L. and Vale, R. D. (2004). Molecular dissection of the roles of nucleotide binding and hydrolysis in dynein's AAA domains in *Saccharomyces cerevisiae*. *Proc. Natl. Acad. Sci. USA*, **101**(6), pp. 1491–1495.

55. Reck-Peterson, S. L., Yildiz, A., Carter, A. P., Gennerich, A., Zhang, N. and Vale, R. D. (2006). Single-molecule analysis of dynein processivity and stepping behavior. *Cell*, **126**(2), pp. 335–348.

56. Reiner, O., Carrozzo, R., Shen, Y., Wehnert, M., Faustinella, F., Dobyns, W. B., Caskey, C. T. and Ledbetter, D. H. (1993). Isolation of a Miller-Dieker lissencephaly gene containing G protein beta-subunit-like repeats. *Nature*, **364**(6439), pp. 717–721.

57. Roberts, A. J., Numata, N., Walker, M. L., Kato, Y. S., Malkova, B., Kon, T., Ohkura, R., Arisaka, F., Knight, P. J., Sutoh, K. and Burgess, S. A. (2009). AAA+ Ring and linker swing mechanism in the dynein motor. *Cell*, **136**(3), pp. 485–495.

58. Ross, J. L., Wallace, K., Shuman, H., Goldman, Y. E. and Holzbaur, E. L. (2006). Processive bidirectional motion of dynein-dynactin complexes *in vitro*. *Nat. Cell Biol*., **8**(6), pp. 562–570.

59. Ross, J. L., Shuman, H., Holzbaur, E. L. and Goldman, Y. E. (2008). Kinesin and dynein-dynactin at intersecting microtubules: motor density affects dynein function. *Biophys. J*., **94**(8), pp. 3115–3125.

60. Runnegar, M. T., Wei, X. and Hamm-Alvarez, S. F. (1999). Increased protein phosphorylation of cytoplasmic dynein results in impaired motor function. *Biochem. J*., **342 (1)**, pp. 1–6.

61. Sasaki, S., Shionoya, A., Ishida, M., Gambello, M. J., Yingling, J., Wynshaw-Boris, A. and Hirotsune, S. (2000). A LIS1/NUDEL/cytoplasmic dynein heavy chain complex in the developing and adult nervous system. *Neuron*, **28**(3), pp. 681–696.

62. Schroer, T. A. and Sheetz, M. P. (1991). Two activators of microtubule-based vesicle transport. *J. Cell Biol.*, **115**(5), pp. 1309–1318.

63. Schroer, T. A. (2004). Dynactin, *Annu. Rev. Cell Dev. Biol.*, **20**, pp. 759–779.

64. Sheeman, B., Carvalho, P., Sagot, I., Geiser, J., Kho, D., Hoyt, M. A. and Pellman, D. (2003). Determinants of *S. cerevisiae* dynein localization and activation: implications for the mechanism of spindle positioning. *Curr. Biol.*, **13**(5), pp. 364–372.

65. Shima, T., Imamula, K., Kon, T., Ohkura, R. and Sutoh, K. (2006). Head-head coordination is required for the processive motion of cytoplasmic dynein, an AAA+ molecular motor. *J. Struct. Biol.*, **156**(1), pp. 182–189.

66. Shubeita, G. T., Tran, S. L., Xu, J., Vershinin, M., Cermelli, S., Cotton, S. L., Welte, M. A. and Gross, S. P. (2008). Consequences of motor copy number on the intracellular transport of kinesin-1-driven lipid droplets. *Cell*, **135**(6), pp. 1098–1107.

67. Silvanovich, A., Li, M. G., Serr, M., Mische, S. and Hays, T. S. (2003). The third P-loop domain in cytoplasmic dynein heavy chain is essential for dynein motor function and ATP-sensitive microtubule binding. *Mol. Biol. Cell*, **14**(4), pp. 1355–1365.

68. Sims, P. A. and Xie, X. S. (2009). Probing dynein and kinesin stepping with mechanical manipulation in a living cell. *ChemPhysChem,* **10**(9-10), pp. 1511–1516.

69. Soppina, V., Rai, A. K., Ramaiya, A. J., Barak, P. and Mallik, R. (2009). Tug-of-war between dissimilar teams of microtubule motors regulates transport and fission of endosomes. *Proc. Natl. Acad. Sci. USA*, **106**(46), pp. 19381–19386.

70. Susalka, S. J. and Pfister, K. K. (2000). Cytoplasmic dynein subunit heterogeneity: implications for axonal transport. *J. Neurocytol.*, **29**(11–12), pp. 819–829.

71. Svoboda, K. and Block, S. M. (1994). Force and velocity measured for single kinesin molecules. *Cell*, **77**(5), pp. 773–784.

72. Tai, C. Y., Dujardin, D. L., Faulkner, N. E. and Vallee, R. B. (2002). Role of dynein, dynactin, and CLIP-170 interactions in LIS1 kinetochore function. *J. Cell Biol.*, **156**(6), pp. 959–968.

73. Tarricone, C., Perrina, F., Monzani, S., Massimiliano, L., Kim, M. H., Derewenda, Z. S., Knapp, S., Tsai, L. H. and Musacchio, A. (2004). Coupling PAF signaling to dynein regulation: structure of LIS1 in complex with PAF-acetylhydrolase. *Neuron*, **44**(5), pp. 809–821.

74. Toba, S., Watanabe, T. M., Yamaguchi-Okimoto, L., Toyoshima, Y. Y. and Higuchi, H. (2006). Overlapping hand-over-hand mechanism of single molecular motility of cytoplasmic dynein. *Proc. Natl. Acad. Sci. USA*, **103**(15), pp. 5741–5745.

75. Ueno, H., Yasunaga, T., Shingyoji, C. and Hirose, K. (2008). Dynein pulls microtubules without rotating its stalk. *Proc. Natl. Acad. Sci. USA*, **105**(50), pp. 19702–19707.

76. Vale, R. D. (2003). The molecular motor toolbox for intracellular transport. *Cell*, **112**(4), pp. 467–480.

77. Vale, R. D., Schnapp, B. J., Mitchison, T., Steuer, E., Reese, T. S. and Sheetz, M. P. (1985). Different axoplasmic proteins generate movement in opposite directions along microtubules *in vitro*. *Cell*, **43**(3 Pt 2), pp. 623–632.

78. Vallee, R. B., Wall, J. S., Paschal, B. M. and Shpetner, H. S. (1988). Microtubule-associated protein 1C from brain is a two-headed cytosolic dynein. *Nature*, **332**(6164), pp. 561–563.

79. Walter, W. J., Brenner, B. and Steffen, W. (2010). Cytoplasmic dynein is not a conventional processive motor. *J. Struct. Biol*., **170**(2), pp. 266–269.

80. Wang, Z., Khan, S. and Sheetz, M. P. (1995). Single cytoplasmic dynein molecule movements: characterization and comparison with kinesin. *Biophys. J.*, **69**(5), pp. 2011–2023.

81. Watanabe, T. M., Sato, T., Gonda, K. and Higuchi, H. (2007). Three-dimensional nanometry of vesicle transport in living cells using dual-focus imaging optics. *Biochem. Biophys. Res. Commun.*, **359**(1), pp. 1–7.

82. Watanabe, T. M. and Higuchi, H. (2007). Stepwise movements in vesicle transport of HER2 by motor proteins in living cells. *Biophys. J.*, **92**(11), pp. 4109–4120.

83. Waterman-Storer, C. M., Karki, S. and Holzbaur, E. L. (1995). The $p150^{Glued}$ component of the dynactin complex binds to both microtubules and the actin-related protein centractin (Arp-1). *Proc. Natl. Acad. Sci. USA*, **92**(5), pp. 1634–1638.

84. Xiang, X., Osmani, A. H., Osmani, S. A., Xin, M. and Morris, N. R. (1995). NudF, a nuclear migration gene in *Aspergillus nidulans*, is similar to the human LIS-1 gene required for neuronal migration. *Mol. Biol. Cell*, **6**(3), pp. 297–310.

85. Yamada, M., Toba, S., Yoshida, Y., Haratani, K., Mori, D., Yano, Y., Mimori-Kiyosue, Y., Nakamura, T., Itoh, K., Fushiki, S., Setou, M., Wynshaw-Boris, A., Torisawa, T., Toyoshima, Y. Y. and Hirotsune, S. (2008). LIS1 and NDEL1 coordinate the plus-end-directed transport of cytoplasmic dynein. *EMBO J.*, **27**(19), pp. 2471–2483.

86. Yildiz, A., Forkey, J. N., McKinney, S. A., Ha, T., Goldman, Y. E. and Selvin, P. R. (2003). Myosin V walks hand-over-hand: single fluorophore imaging with 1.5-nm localization. *Science*, **300**(5628), pp. 2061–2065.

87. Yildiz, A., Tomishige, M., Vale, R. D. and Selvin, P. R. (2004). Kinesin walks hand-over-hand. *Science*, **303**(5658), pp. 676–678.

88. Yildiz, A., Tomishige, M., Gennerich, A. and Vale, R. D. (2008). Intramolecular strain coordinates kinesin stepping behavior along microtubules. *Cell*, **134**(6), pp. 1030–1041.